normal crystal structure would be at variance with such an observation.

There is a remarkable similarity emerging between our postulated structure and observed morphology and that of the fringed micelle thought in the past to be characteristic of crystal structures in polymers. A fully ordered structure was associated with the fringed micelle, but an alternative way of describing our high pressure phase could be as fringed micelles in which the chains have packed together in an approximately uniaxial fashion. We are, of course, unable to comment on the molecular structure of the end surfaces.

The reported diffraction pattern for the high pressure phase in polyethylene [5] is consistent with our proposed model, even though it was interpreted as a fully-ordered hexagonal phase. In shape, the species in both polymers are remarkably similar although the nucleation densities and sizes are very different. Indeed, it has been suggested [9], on the basis of *in situ* crystal growth studies, that the phase in polyethylene is liquid crystalline in nature. The suggestion made was that a nematic was the correct classification, but this would not be consistent with the X-ray data [5].

We would suggest that in view of the remarkably similar crystalline and morphological structures there is a possibility that this disordered hexagonal or liquid crystalline phase may be a general occurrence in crystalline polymers at sufficiently high pressures if nucleation and growth of lamellar crystals is severely inhibited.

Acknowledgement

We would like to thank the Science Research Council for financial support.

References

1. P. J. PHILLIPS and E. H. ANDREWS, *J. Polymer Sci. B* **10** (1972) 321.
2. B. C. EDWARDS and P. J. PHILLIPS, *Polymer* **15** (1974) 491.
3. D. C. BASSETT and B. TURNER, *Phil. Mag.* **29** (1974) 285.
4. *Idem, ibid* **29** (1974) 925.
5. D. C. BASSETT, S. BLOCK and G. J. PIERMARINI, *J. Appl. Phys.* **45** (1974) 4146.
6. A. SKOULIOS, *Adv. Coll. Interface Sci.* **1** (1967) 79.
7. G. H. BROWN, J. W. DOANE and V. D. NEFF, "A Review of the Structure and Properties of Liquid Crystals" (Butterworths, London, 1971).
8. R. DE GENNES, "Physics of Liquid Crystals" (Oxford University Press, 1974).
9. M. YASUNIWA and T. TAKEMURA, *Polymer* **15** (1974) 661.
10. P. J. PHILLIPS and B. C. EDWARDS, *J. Polymer Sci.* to be published.

Received 4 December 1974
and accepted 27 January 1975

B. C. EDWARDS*
P. J. PHILLIPS†
Department of Materials
Queen Mary College,
University of London, UK

*Present address: Metallurgy Division, AERE, Harwell, Oxon., UK.
†Present address: Department of Chemical Engineering, State University of New York at Buffalo, Buffalo, NY 14214, USA.

On the mode of chipping fracture in brittle solids

Chipping processes in brittle solids, despite their unquestionable relevance to a diversity of technologies from ceramics finishing to geological engineering, are not well understood at the fundamental level. Some recent studies of microfracture patterns beneath standard hardness indenters do, however, provide some insight into the problem [1, 2], and it is our objective here to indicate how this insight may be applied to construct a physical model of chipping fracture. Essentially, the picture which emerges is that depicted in Fig. 1. (i) Upon *loading* the indenter, a confined zone of irreversible (plastic) deformation forms about any sharp points or corners (thereby accounting for the residual hardness impression), from which "median vent" cracks first initiate and subsequently propagate radially outward along suitable planes of symmetry (e.g. as defined by the diagonals of a pyramid indenter, or by preferred cleavage planes) containing the contact axis. (ii) Upon *unloading* the indenter, the median vents close up but, just prior to complete removal, "lateral vent" cracks initiate and extend laterally from the deformation zone toward the specimen surface. Of the two types of cracking, it is clearly the second which relates more directly to brittle chipping.

However, up to now a detailed fracture

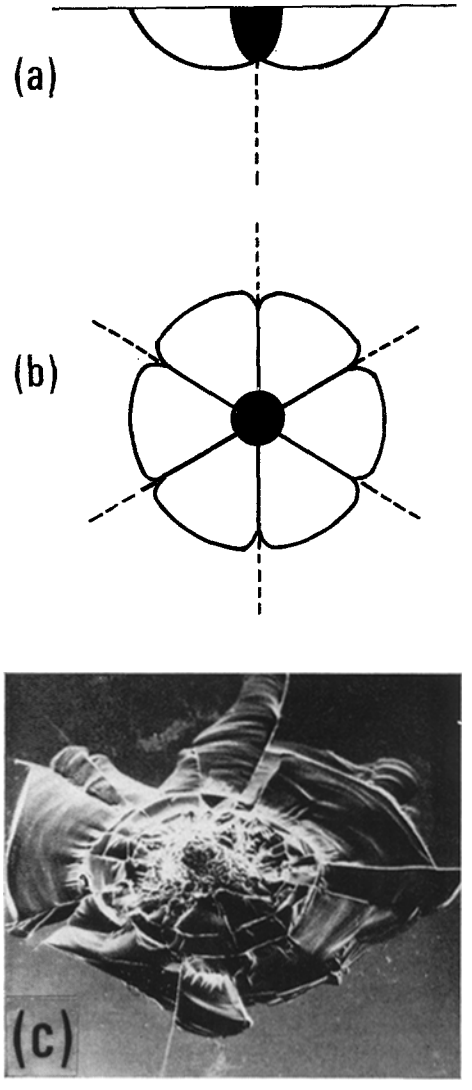

Figure 1 Fracture geometry beneath sharp indenter. Central deformation zone shown as dark region, median vent cracks as broken lines, lateral vent cracks as heavy lines. (a) Section view schematic, (b) plan view schematic, (c) surface view of fused silica indented with sharp, irregular particle (SEM, field width 3 mm).

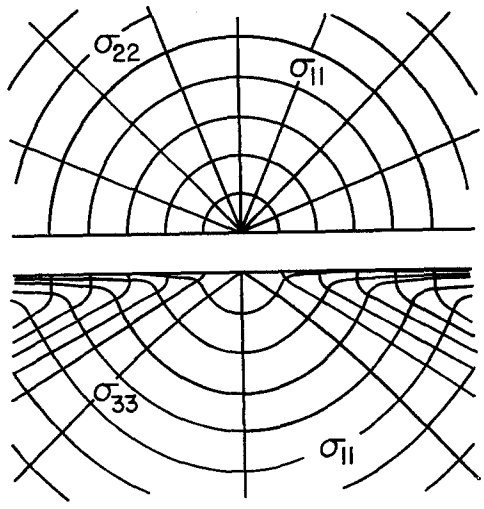

Figure 2 Stress trajectories (curves whose tangent indicates direction of principal stress) for Boussinesq field, showing half-surface view (top) and section view (bottom). Cone cracks initiate from incipient surface flaws and propagate everywhere orthogonally to σ_{11} (tensile outside contact area), median vents initiate from central deformation zone and propagate orthogonally to σ_{22} (tensile below contact zone), lateral vents initiate from deformation zone and propagate nearly orthogonally to σ_{33} (compressive everywhere, but tensile if applied load reversed).

mechanics analysis has been attempted only for the median vent system. This system is relatively well defined, since the indentation stress field, which uniquely determines the extent of crack growth [1], can reasonably be represented in terms of the classical Boussinesq field for normal point loading [2, 3]. On the basis of the fundamental Griffith energy-balance condition for fracture [4], it may readily be argued that brittle cracks will generally tend to follow trajectories of the lesser principal stresses within the indentation field, such that the path maintains near-orthogonality to a component of major tension: the best studied illustration of this principle is the Hertzian cone crack [5, 6] which, in the absence of any deformation-induced nucleation centre, initiates from an incipient surface flaw and flares downward into the specimen. In the scheme of Fig. 2, in which the principal stresses are defined such that $\sigma_{11} \geqslant \sigma_{22} \geqslant \sigma_{33}$ (positive values denoting tension) nearly everywhere, median vent geometry may be specified in terms of families of σ_{11} and σ_{33} trajectories, cone crack geometry in terms of families of σ_{22} and σ_{33} trajectories.

The conditions under which the lateral vents form are, unfortunately, less easily modelled. Since the lateral system operates only as the indenter is withdrawn from the specimen surface, it is evident that the driving force for propagation must originate from some residual stress field associated with the irreversible deformation zone. This conclusion is substantiated by microscopic investigation of the damage patterns as a function of indenter

geometry (e.g. "sharp" or "blunt"): in general, the extent of lateral venting is found to increase markedly with expanding zone size. A graphic illustration of the effect is obtained by loading a soda-lime glass plate with a small (1 mm diameter) spherical indenter: at comparatively low load the contact is elastic, and the only fracture is that of cone cracking, whereas at higher load some plasticity develops beneath the penetrating sphere, and lateral venting becomes evident in the unloaded plate [1]. A related effect was reported by Culf [7], who observed otherwise regular cone cracks in glass to deflect upward ("hat brim" effect) upon sudden release of the indenter load. Culf also observed considerable residual stress birefringence in association with this phenomenon, over distances large compared with the scale of the deformation zone itself. That residual stresses exist about hardness impressions in most brittle materials has been amply demonstrated by a number of strain-sensitive techniques [8]. That these stresses can also be moderately long-range in nature is seen most clearly in the distances over which relaxation by plastic flow (e.g. dislocation loop punching) occurs in annealing experiments [9]. Neither the existence nor the intensity of the residual elastic fields should come as any surprise, for the stress levels achieved beneath the indenter in hardness tests on highly brittle solids tend to be of the order of the intrinsic bond strength of the structure [10, 11], and the relief of these high stresses would ideally require the impressed region to restore completely to its original unstrained state.

These observations, coupled with a re-examination of the Boussinesq field, provide us with a working model upon which to base an analysis of lateral vent formation. We note that the lateral vents extend in all cases on surfaces closely delineated by families of σ_{11} and σ_{22} trajectories in Fig. 2 (although the paths are modified somewhat by the deformation zone itself, and by free surfaces, including any pre-existing median vents or cone cracks); it is as if the applied load were actually reversed upon indenter withdrawal, so that the σ_{33} stress normal to the lateral vent becomes the dominant component of tension in the field. Of course, it is physically meaningless to associate a reversed applied load with a surface in the unloaded state, but an effectively similar net result may obtain if the deformation zone were to act as a centre of contraction with respect to the surrounding

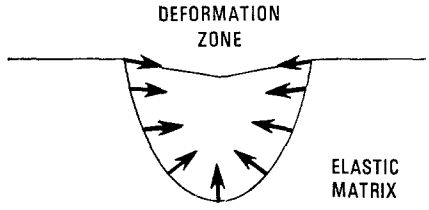

Figure 3 Schematic representation of distribution of mismatch tractions at boundary between central deformation zone and surrounding elastic matrix, at indenter withdrawal.

elastic matrix. This effect is depicted schematically in Fig. 3. The distribution of stresses at the zone boundary must inevitably depend strongly on the nature of the irreversible deformation (which itself remains an issue of some controversy [11, 12]). Nevertheless, one can proceed by making reasonable assumptions as to this distribution (e.g. that the tractions are of constant magnitude, and are directed such that the net force is zero), and evaluate the residual field in the matrix by taking expressions for the stresses due to elemental point forces (e.g. Mindlin [13]) and integrating around the boundary. One may then construct a stress trajectory pattern for the field, in analogy to Fig. 2, and thereby trace out prospective fracture paths from the deformation zone. Full details of such calculations will be discussed elsewhere; we simply report here that the predicted paths do indeed curve toward the specimen surface in essentially the manner shown in Fig. 1.

The scope of the present model extends well beyond the establishment of a suitable basis for evaluating an "index of brittleness" in standard hardness testing [14]. It provides physical insight into a number of seemingly unrelated phenomena in brittle solids.

(i) *Strength degradation.* Surface damage introduced into a brittle surface as a result of contact (either static or impact) with hard particles constitutes a potential source of weakness. The mechanics of the damage process may be conveniently simulated in a simple indentation test [15].

(ii) *Glass cutting.* A glass cutter's wheel is designed to produce a continuous "trailing" median vent as a linear starting crack for subsequent plate fracture in flexure. However, lateral venting invariably occurs in the wake of

the moving "indenter", thereby damaging the edges of the final cut. Clearly, the need here is for a means of suppressing the chipping mode.

(iii) *Surface removal processes.* Individual chipping events in the machining, drilling, grinding, abrasion, erosion and wear of brittle surfaces in general (e.g. ceramics, gemstones, rocks) are of the type depicted in Fig. 1 [1]. By summing over an appropriate distribution of such microscopic events, it should be possible to describe macroscopic surface removal parameters at a fundamental level.

(iv) *Geophysical impact phenomena.* Meteorite-induced craters ranging in scale from geological land masses [16] to lunar fines [17] bear a resemblance to the damage pattern in Fig. 1 which can only be described as striking. While thermal and stress-wave effects associated with the high-velocity impacts are undoubtedly important factors in these cases [18], the possible role of residual stresses about the central "deformation zone" in determining crater morphology may warrant further attention.

References

1. B. R. LAWN and T. R. WILSHAW, *J. Mater. Sci.* **10** (1975) 1049.
2. B. R. LAWN and M. V. SWAIN, *ibid* **10** (1975) 113.
3. J. BOUSSINESQ, "Application des Potentiels a l'Etude de l'Equilibre et du Mouvement des Solides Elastiques" (Gauthier-Villars, Paris, 1885). Discussed in S. P. TIMOSHENKO and J. N. GOODIER, "Theory of Elasticity" (McGraw-Hill, New York, 1970) pp. 398-402.
4. A. A. GRIFFITH, *Phil. Trans. Roy. Soc. Lond.* **A211** (1920) 163.
5. H. HERTZ, *J. Reine Angew. Math.* **92** (1881) 156; *Verhandlungen des Vereins zur Beforderung des Gewerbe Fleisses* **61** (1882) 449. Reprinted in English, in "Hertz's Miscellaneous Papers" (Macmillan, London, 1896) Chs. 5, 6.
6. F. C. FRANK and B. R. LAWN, *Proc. Roy. Soc. Lond.* **A299** (1967) 291.
7. C. J. CULF, *J. Soc. Glass. Tech.* **41** (1957) 157.
8. B. J. HOCKEY, in "The Science of Hardness Testing and its Research Applications", Symposium Proceedings, edited by J. H. Westbrook and H. Conrad (American Society for Metals, Metals Park, Ohio, 1973) Ch. 3.
9. R. WAGATSUME, K. SUMINO, W. UCHIDA and S. YAMAMOTO, *J. Appl. Phys.* **42** (1971) 222.
10. A. KELLY, "Strong Solids" (Clarendon, Oxford, 1966).
11. M. J. HILL and D. J. ROWCLIFFE, *J. Mater. Sci.* **9** (1974) 1569.
12. F. M. ERNSBERGER, *Ann. Rev. Mat. Sci.* **2** (1972) 529.
13. R. D. MINDLIN, *Physics* **7** (1936) 195.
14. J. H. WESTBROOK, in "The Science of Hardness Testing and its Research Applications", Symposium Proceedings, edited by J. H. Westbrook and H. Conrad (American Society for Metals, Metals Park, Ohio, 1973) pp. 491-4.
15. A. G. EVANS, *J. Amer. Ceram. Soc.* **56** (1973) 405.
16. A. NADAI, "Theory of Flow and Fracture of Solids" (McGraw-Hill, New York, 1963) pp. 247-9.
17. J. L. CARTER and I. D. MacGREGOR, *Proc. Apollo 11 Lunar Sci. Conf.* **1** (1970) 247.
18. J. F. VEDDER and J.-C. MANDEVILLE, *J. Geophys. Res.* **79** (1974) 3247.

Received 31 January
and accepted 3 February 1975

B. R. LAWN
Institute for Materials Research,
National Bureau of Standards,
Washington, D.C., USA
M. V. SWAIN
Martin Marietta Laboratories,
1450 South Rolling Road,
Baltimore, Maryland, USA
K. PHILLIPS,
Division of Materials Science
School of Applied Sciences,
University of Sussex, UK

Using electron/atom ratio in titanium alloy design

A correlation between beta phase stability in titanium and zirconium-base alloys and solute valence has been noted [1, 2]. Such a correlation, if sufficiently precise, could prove quite valuable in the design of strain transformable beta titanium alloys, since these alloys show optimum properties at alloy contents just adequate to insure complete retention of a metastable beta phase on quenching from above the beta transus [3]. Information on the microstructural characteristics of a series of beta titanium alloys quenched from above the beta transus, available from a prior investigation [3], was used to determine how well the observed microstructural characteristics of these alloys correlated with the computed electron/atom ratio.

An initial question which arose in performing this analysis was the proper choice of valence for